Vibrio cholerae chromosome 2 copy number is controlled by the methylation-independent binding of its monomeric initiator to the chromosome 1 *crtS* site

Francisco de Lemos Martins[1,2,†], Florian Fournes[1,2,†], Maria-Vittoria Mazzuoli[1,2], Didier Mazel[1,2,*] and Marie-Eve Val [1,2,*]

[1]Bacterial Genome Plasticity, Genomes & Genetics Department, Institut Pasteur, Paris 75015, France and
[2]UMR3525, Centre National de la Recherche Scientifique, Paris 75015, France

ABSTRACT

Bacteria contain a primary chromosome and, frequently, either essential secondary chromosomes or dispensable megaplasmids of plasmid origin. Incoming plasmids are often poorly adapted to their hosts and their stabilization requires integration with the host's cellular mechanisms in a process termed domestication. All *Vibrio*, including pathogenic species, carry a domesticated secondary chromosome (Chr2) where replication is coordinated with that of the primary chromosome (Chr1). Chr2 replication is triggered by the replication of an intergenic sequence (*crtS*) located on Chr1. Yet, the molecular mechanisms by which *crtS* replication controls the initiation of Chr2 replication are still largely unknown. In this study, we show that *crtS* not only regulates the timing of Chr2 initiation but also controls Chr2 copy number. We observed and characterized the direct binding of the Chr2 initiator (RctB) on *crtS*. RctB binding to *crtS* is independent of its methylation state. RctB molecules, which naturally form dimers, preferentially bind to *crtS* as monomers, with DnaK/J protein chaperones shown to stimulate binding of additional RctB monomers on *crtS*. In this study, we addressed various hypothesis of how replication of *crtS* could trigger Chr2 replication and provide new insights into its mode of action.

INTRODUCTION

Nearly 10% of bacteria harbor large secondary replicons being classified either as chromids or as megaplasmids (1,2). Chromids (also called secondary chromosomes) encode essential core genes and have nucleotide and codon compo-sitions close to the chromosome, suggesting that they have evolved together for hundreds of millions of years to become domesticated (2,3). Chromids replicate using plasmid-like mechanisms indicating that they originated from plasmids or megaplasmids (2). Since plasmids are frequently maladapted to a new genetic background, their stabilization in the genome must require adaptation to the host cell cycle and physiology. Replication is primarily regulated at the initiation step (4) and plasmid eventually become domesticated as *bona fide* secondary chromosomes through cell-cycle synchronized replication controls. As of today, most of our knowledge on the conjoint management of chromosomes and chromids comes from the bacterial model *Vibrio cholerae*, which has a genome divided over a main chromosome (Chr1) of 3 Mb and a chromid (Chr2) of 1 Mbp (5–7).

Each of the two replicons encodes for its own initiator protein to start replication at unalike replication origins (8). Chr1 replication initiation is performed by DnaA the ubiquitous chromosome replication initiator in bacteria (9), and the replication origin of *V. cholerae* Chr1 (*ori1*) is fairly similar to the canonical *Escherichia coli* chromosomal origin (*oriC*) (8,10). *ori1* contains five DnaA binding sites (DnaA boxes), an IHF binding site and an AT-rich region for replication initiation. In addition, Chr1 *ori1* contains several GATC sites for methylation by DNA adenine methyltransferase (Dam) which regulates the timing of subsequent re-initiation through sequestration of hemi-methylated sites by SeqA (11,12). On the other hand, Chr2 replication initiation is triggered by a *Vibrio*-specific factor called RctB, and Chr2 replication origin (*ori2*) is closely related to the one of iteron-type plasmids (8). *ori2* can be divided in two regions: a minimum origin of replication (Figure 1A, (+)) and a region of regulation of Chr2 replication (Figure 1A, (−)). The minimum origin of replication contains the *rctB* encoding gene and six repeated 12-mers (iterons) onto which RctB binds to promote replication initiation with the unwinding of a contiguous AT-rich sequence (13). It also con-

tains putative IHF and DnaA binding sites, the latter being required for replication at *ori2* (14,15). The *ori2* regulatory region contains a transcribed but non-translated ORF (*rctA*) and two types of RctB binding sites: five regulatory iterons and two 39-mer motifs, one of which is found in *rctA* (16). RctB binds efficiently to the 39-mer motifs where it serves as a negative regulator of *ori2* initiation (16,17). This inhibitory activity is mainly achieved by origin handcuffing which consists in bridging 39-mers with iterons via RctB (7,16–18). *ori2* handcuffing by a 39-mer is a strong inhibitor and several mechanisms can counteract 39-mer replication inhibitory activity. For example, the transcription of *rctA* interferes with RctB binding to 39-mer (18) and ParB2 competes with RctB to bind to 39-mers (19). Adjacent to *ori2* are found ParA2 and ParB2 encoding genes (Figure 1A) that are related to plasmid partitioning systems and which are crucial for Chr2 maintenance (20). Plasmid partitioning systems consist of two proteins, ParA and ParB, and *cis*-acting centromere-like sites, *parS*. One parB2 binding sites is located within *ori2*, in *rctA* (Figure 1A, *parS2-B*). ParB2 spreads from *parS2-B* into the *rctA* 39-mer and interferes with RctB 39-mer-binding replication inhibitory activity (19). ParB2 also binds directly to a 39-mer motif outside *rctA* without requiring initial binding to a *parS2* site and out-compete RctB binding (19). On the other hand, binding of RctB to *rctA* activates *parAB2* expression (21). These binding fluctuations show how chromosome replication and origin segregation can be intimately intertwined. In addition to the *ori2* binding regions, RctB binds within a 74 kb DNA stretch containing five iterons and one 39-mer motif, located 40 kb away from *ori2* (22). This locus negatively regulates *ori2* replication and was suggested to be analogous of the *E. coli datA* initiator titration locus (23,24).

RctB is a 658 AA protein with four domains. Its central region (domains 2 and 3) is structurally homologous to iteron plasmid initiators while its outer domains (domains 1 and 4) are unique (25). RctB has three identified DNA binding surfaces in domains 1, 2 and 3 and the protein can adopt a monomeric or a dimeric form (25). Its dimer interface is mediated by domain 2 and mutations impairing its dimerization such as RctB$_{D314P}$, have been identified (25). Domain 4 could be involved in protein/protein interactions and promote RctB cooperative binding (17,25). RctB was reported to bind as a monomer or as a dimer onto iterons but only as a monomer on 39-mers (17,26). RctB is remodeled by chaperones DnaJ and DnaK which promote the binding of RctB to both iterons and 39-mers (17). DnaK specifically interacts with RctB to promote its monomerization but also to remodel RctB monomers (27).

Chromosomes ensure a single round of replication per cell cycle (28). This is not the case for iteron-type plasmids, which replicate several times per cell cycle (7). Despite its plasmid-like vestiges, Chr2 replication is restricted to only once per cell cycle. All iterons in *ori2* have a GATC site that needs to be fully methylated in order to bind RctB (29) while plasmid iterons lack GATC sites. Dam methylation is therefore essential for Chr2 replication (30). In contrast, RctB binding to the 39-mer motifs do not require methylation (31). Dam regulation of Chr2 replication offered some clues as to how Chr2 replication is limited to once per cell cycle (31).

In *V. cholerae*, the timing of Chr1 and Chr2 initiations is coordinated in such a way that they terminate replicating at the same time (32). Chr1 initiates at the onset of the replication period while initiation of Chr2 is delayed and occurs when two-thirds of the replication period has completed (32). In fact, Chr2 monitors the replication status of Chr1 to time its own replication via a non-coding locus on Chr1, called *crtS* (Chr2 replication triggering site) (33). This locus was originally found by the ChIP-chip of RctB on *V. cholerae* genome (22) and its critical role in the coordinated timing of Chr1 and Chr2 replication was only revealed later (33). Indeed, Chr2 initiates replication only when *crtS* has been replicated (33). By fluorescence microscopy, using mutants with two chromosomal copies of *crtS*, we observed that the duplication of one *crtS* triggers the firing of only one *ori2* suggesting that Chr2 initiation firing may necessitate a direct interaction between *crtS* and *ori2* (33). *crtS* is an intergenic sequence located ∼690 Kb downstream of *ori1* on Chr1 (between VC764 and VC765 genes), conserved in the *Vibrionaceae* family (22,34). Its sequence shows no homology to previously described RctB binding sites, i.e. iterons or 39-mers. *crtS* contains an AT-rich stretch, a putative DnaA box and several conserved GATC sites. Deletion of *crtS* severely impairs growth and is associated with cell filamentation and Chr2 loss (33). This phenotype was shown to be directly linked to improper regulation/activation of Chr2 replication (33). The presence of a *crtS*-containing plasmid in *E. coli* enhances the replication of an *ori2*-driven plasmid (15,22). Serial deletions of a DNA fragment containing *crtS* in a plasmid showed that the replication-enhancing activity of an *ori2*-driven plasmid in *E. coli* could be narrowed down to a 70-mer site (chrI-9) (22). Surprisingly, the direct binding of RctB on *crtS* could never be obtained by electrophoretic mobile shift assay (EMSA) (22). RctB binding site on *crtS* was inferred by primer extension mapping of a DnaseI footprinting only when *crtS* was contained on a supercoiled plasmid (22). Seven protected bases were found within the 70-mer to have an important role in *crtS* activity (22). These data suggested that RctB binding to *crtS* is weak and that other factors might be required to promote its binding. It was shown that *crtS*-containing plasmids increased RctB affinity to iterons, decreased RctB affinity to 39-mers and also abolished the requirement for the DnaK/J chaperones, which are normally required to promote initiation at *ori2* in *E. coli* (22). Baek *et al.* suggested that *crtS* may act like a DNA chaperone to remodel RctB which would alter its binding to both iterons and 39-mers. However this remodeling would act differently than DnaK/J, which increase RctB binding to both iterons and 39-mers.

The molecular mechanism by which *crtS* controls the initiation of Chr2 replication is still largely unknown. Chr2 initiation requires *crtS* replication, meaning that either DNA alterations caused by the passage of the replication fork across *crtS* or the doubling in copy number of *crtS* after duplication triggers Chr2 replication (33). In a previous work, we showed that in mutants with two chromosomal copies of *crtS*, the majority of newborn cells display an unbalanced chromosome ratio with two *ori2* and only one *ori1* (33). This suggested that having two copies of *crtS* is enough to trigger Chr2 replication initiation. On the other hand, the replica-

tion of *crtS* generates transiently hemi-methylated GATC sites that could affect RctB binding and send a signal to trigger Chr2 replication. In this work, we combined *in silico*, *in vivo* and *in vitro* approaches to study the genetic determinants enclosed within the *crtS* sequence, to characterize the binding parameters of RctB on *crtS* and to inspect the involvement of other factors (Dam methylation, ParAB2, DnaA, DnaK/J) in the *crtS*-RctB-*ori2* replication system.

We show that *crtS* regulates not only the timing of Chr2 initiation but also its copy number. We defined the minimum *crtS* functional sequence in *V. cholerae* and found out that it significantly differs from the 70-mer previously found in *E. coli*. We demonstrated *in vitro* that RctB binds to a linear *crtS* site independently of its methylation state. We confirmed that DnaA binds to *ori2* but not *crtS*, rejecting the existence of DnaA box in *crtS*. We further show that RctB binds specifically to all its sites (iterons, 39-mer, *crtS*) preferentially under its monomeric form. We observed that DnaK/J promotes both RctB monomerization and the binding of additional RctB monomers. Our results suggest that RctB molecules oligomerize on DNA after their initial specific binding to their site. We propose that RctB molecules oligomerize on Chr1 from *crtS* (nucleation point), and that upon the passage of the replication fork, RctB is somehow activated to trigger Chr2 replication.

MATERIALS AND METHODS

Bacterial strains and plasmids

Bacterial strains, plasmids and primers used in this study are listed in Supplementary Tables S1–S4. Details are given in the Supplementary Material.

Genome editing by co-transformation

Insertions of point mutations in *crtS* were performed according to the MuGENT procedure described in (35). Details are given in the Supplementary Material.

Tn7 transposition

crtS sites of various lengths were transposed into the unique Tn7 attachment site (*attTn7*) of *V. cholerae*, located near VC487 on Chr1. Briefly, *crtS* sites were inserted between Tn7 recombination sites contained in a shuttle vector (Supplementary Figure S1, pTn7::*crtS*) (Supplementary Table S1, pMVM5). *crtS* containing shuttle vectors were then conjugated along with a helper plasmid (Supplementary Figure S1, pMVM1) in the recipient strain, MV250. pMVM1 encodes for TnsABCD that promote transposition into *attTn7*, at a high frequency (36). The recipient *V. cholerae* strain, MV250, has its native *crtS* site flanked by *frt* recombination sites. Once another copy of *crtS* was inserted in *attTn7*, the native *crtS* was excised using the Flippase (Flp) encoded on pMP108 (Supplementary Table S1). The native *crtS* site was always deleted last to avoid the rapid acquisition of compensatory mutations as observed in (33).

Digital PCR quantification of DNA loci

The absolute quantification of (*ori1*, *ori2*) and (*oriC*, pORI2) was performed in multiplex by digital PCR (Stilla

Technologies, Villejuif, France) and used to generate ratios (*ori2*/*ori1*, pORI2/*oriC*) (37). Primers and probes are listed in Supplementary Table S2. Details are given in the Supplementary Material.

Plasmid stability assay

Plasmid stability assays were performed by growing bacteria in MH at 37°C under agitation for 60 or 80 generations. Liquid cultures grown in absence of antibiotic selection were spread every 10 or 20 generations onto MH and MH containing chloramphenicol agar plates to determine the percentage of cells harboring plasmid (Supplementary Figure S2). Details are given in the Supplementary Material.

Proteins purification

pET32b-derived expression plasmids were used to transform *E.coli* BL2-D3 strain (Supplementary Table S1). The resulting strains were grown in LB to an OD_{600} of 0.6. After 42°C heat chock, protein expression was performed at 16°C and induced with 0.1mM IPTG for at least 8 h. Lysis was performed in a buffer-P (50 mM Tris–HCl pH 8, 300 mM Nacl, 10% glycerol) complemented with 0.1 mg/ml lysozyme and EDTA free protease inhibitor cocktail (Roche) for 1 h 30 min on ice. After sonication and centrifugation (1 h at 20 000 g), the soluble fraction was submitted to chromatography on nickel (1 ml His-trap column, GE) using an imidazole gradient in buffer-P. The eluted proteins were then subjected to an exclusion dialyze against buffer-S (50 mM Tris–HCl pH 8, 500 mM NaCl, 20% glycerol, 1 mM EDTA, 1 mM DTT). After verification on NuPAGE bis-tris protein gel (Invitrogen), proteins were considered as more than 90% pure and store at -80°C (Supplementary Figure S3).

In vitro experiments

For Electrophoretic Mobile Shift assays (EMSA), the 114-bp *crtS* probe was amplified by PCR and purified by agarose gel electrophoresis (Supplementary Table S3). The methylated DNAs are produced *in vitro* using the *E. coli* Dam methylase following the provided protocol (Biolabs). These subtracts, as the other synthetic oligonucleotides carrying the iteron, 39-mer and *crtS* (Supplementary Table S4), were 5' end labeled with [γ-^{32}P] ATP and T4 DNA polynucleotide kinase. Binding reaction were carried out in a buffer containing 25 mM Tris–HCl pH 8, 250 mM NaCl, 2.5 mM $MgCl_2$, 10% glycerol, 0.5 mM EDTA, 0.5 mM DTT, 0.1 mg/ml BSA, 1 mg of poly(dI-dC) in the presence of 5000 cpm of labeled DNA and the indicated protein concentrations. The reactions were incubated at 30°C for 30 min, analyzed by electrophoresis in 5% polyacrylamide native gel run in 1X TBE, then dried and analyzed with the Typhoon FLA 9500 laser scanner.

For the DNAse I footprinting analysis, 20 000 cpm of 270-bp *crtS* carrying-DNAs (Supplementary Table S3) labeled at the 5' end with [γ-^{32}P] were incubated with various amounts of initiator proteins (RctB, RctB$_{D314P}$) and constant amounts of DnaK$_{Vc}$, DnaJ$_{Vc}$ (5 nM). Reaction was

performed as for the EMSA. After 30 min of incubation at 30°C, the partial digestion of the DNA was initiated by adding DNAse I empirically diluted (1/800). The mixture was incubated 30 s at room temperature and stopped by adding the buffer-Stop (0.4 M sodium acetate, 10 mg/ml ctDNA, 2.5 mM EDTA). DNAs were then ethanol precipitated and re-suspended in 6 μl of loading buffer and separated by electrophoresis in an 8% polyacrylamide denaturing sequencing gel run in 0.6× TBE. Gels were dried and analyzed with the Typhoon FLA 9500 laser scanner.

RESULTS

crtS regulates Chr2 copy number

To better characterize the molecular function of *crtS* on Chr2 maintenance, we reconstituted an artificial replication system in *E. coli* based on *ori2*, RctB and *crtS*. We constructed a set of strains derived from *E. coli* MG1655 carrying up to four chromosomal *crtS* sites (Supplementary Figure S4A) and generated a plasmid, pORI2, which replication in MG1655 solely depends on *ori2*. We performed a plasmid stability assay over 60 generations to follow the loss of pORI2 in function of *crtS* copy number (Supplementary Figure S2). In absence of *crtS*, pORI2 is lost at a high rate of ∼15% per generation while in the presence of only one *crtS*, the loss of pORI2 dropped to 5% per generation (Figure 1B). pORI2 stability tends to increase exponentially as a function of *crtS* copy number (Figure 1C) and was only loss at a rate of 1% per generation when MG1655 contained four *crtS* sites. To understand how *crtS* stabilizes pORI2, we measured the impact of *crtS* on pORI2 copy number. We used multiplex digital PCR (dPCR) to monitor the copy number variation between the *E. coli* chromosome (*oriC* loci) and pORI2 in MG1655 with various number of *crtS* chromosomal sites (37). Genomic DNA was purified from stationary phase cultures where cells are no longer replicating. In these conditions, the *oriC* copy number is equivalent to the chromosome copy number. In absence of *crtS*, pORI2/*oriC* ∼0.5 (Figure 1D), which indicates that half of the population have lost the plasmid. With one *crtS* site, pORI2/oriC ∼2.8, which indicates that cells contain between two and three pORI2 copies. We further observed an exponential increase of pORI2 copy number as a function of *crtS* number (Figure 1D, Supplementary Figure S4A). These results explain the concomitant exponential increase in pORI2 stability since the higher the copy number is, the more likely the two daughter cells will contain a copy of the plasmid. In absence of an active partition system, if plasmids segregate randomly, the probability of having a plasmid-less daughter cell is $2^{(1-\mathrm{CN})}$, where CN is the plasmid copy number. In *E. coli*, *crtS* stabilizes pORI2 by stimulating its replication, which increases its copy number. In *V. cholerae*, we have previously shown that 2 chromosomal copies of *crtS* double *ori2* number of replicating cells leading to cells dividing with one *ori1* and two *ori2* (33). Using dPCR, we measured the copy number variation between Chr1 and Chr2 of non-replicating *V. cholerae* carrying one, two or three *crtS* sites (Supplementary Figure S4B). As expected, Chr2 copy number increased with the number of *crtS* sites (Figure 1E). In WT (VC764), the *ori2*/*ori1* ratio equaled 1 meaning that non-replicating cells have the

same number of Chr1 and Chr2. When a second *crtS* site was added near *ori1* (VC023) or near the terminus of Chr1 (VC963), Chr2 copy number relative to Chr1 increased similarly (*ori2*/*ori1* ∼1.7). When a third *crtS* site was added in the *attTn7* site (VC487), Chr2 copy number relative to Chr1 increased up to 2. Unlike in *E. coli*, Chr2 copy number increases more logarithmically as a function of *crtS* number suggesting that Chr2 copy number is restricted in *V. cholerae* (Supplementary Figure S4B).

crtS and ParAB2 have an additive effect on the control of *ori2* replication

It was shown that *crtS* decreases the binding of RctB to 39-mer (22). This would enhance replication initiation at *ori2* by precluding 39-mer inhibitory effect. Similarly, ParB2 can promote replication at *ori2* by restraining RctB binding to 39-mer (19). We investigated the contribution of both *crtS* and *parAB2* on *ori2* replication to look for potential genetic interactions that would give us new insights into *crtS* mechanism of action. We compared the maintenance of two *ori2*-plasmids, pORI2 and pORI2-*parAB2*, which includes the *ori2* neighbouring *parA2* and *parB2* genes (Figure 1A). We first measured their stability over 80 generations in MG1655 in presence and absence of one chromosomal copy of *crtS* (Figure 2A). Both *crtS* and *parAB2* independently stabilized the plasmid at similar rates (5% and 5.4% plasmid loss per generation, respectively). When both *crtS* and *parAB2* are present, plasmid loss dropped to 0.9% per generation. Because ParAB2 is active in both segregation and replication of Chr2, we measured the copy number of the *ori2*-plasmids to discern the impact of ParAB2 on replication only. Figure 2B shows that *crtS* and *parAB2* independently increase pORI2 copy number. Actually, pORI2 copy number is higher in the presence of *crtS* than in the presence of *parAB2*. The difference between the sum of the individual values obtained with *crtS* and *parAB2* only (2.8 and 1.8, respectively) and the value obtained in the presence of both *crtS* and *parAB2* (4.7) is not significant ($P = 0.4596$ by Student's *t* test), suggesting that the contribution of *crtS* and *parAB2* to pORI2 replication control constitutes an additive effect.

RctB binds to linear *crtS* independently of its methylation state

We characterized the binding of RctB to *crtS* by EMSA. We first checked the binding properties of our purified RctB protein (Supplementary Figure S3) onto iterons and 39-mer containing linear DNA to see if the protein behaved as reported (17). As expected, RctB binding to iterons is Dam-methylation dependent and the binding of RctB to the 39-mer is Dam-methylation independent (Supplementary Figure S5). From previous ChIP-chip of RctB, it was expected that RctB would bind to *crtS*. However, Baek *et al.* reported that no binding of RctB could be directly detected on a 153 bp *crtS*-containing linear or circular DNA (Supplementary Figure S6, ChrI-4) (22). Here, we characterized the binding of RctB on a *crtS*-linear DNA of 114bp encompassing the 70bp minimum functional *crtS* site reported in *E. coli* (Supplementary Figure S6, ChrI-9) (22). In our con-
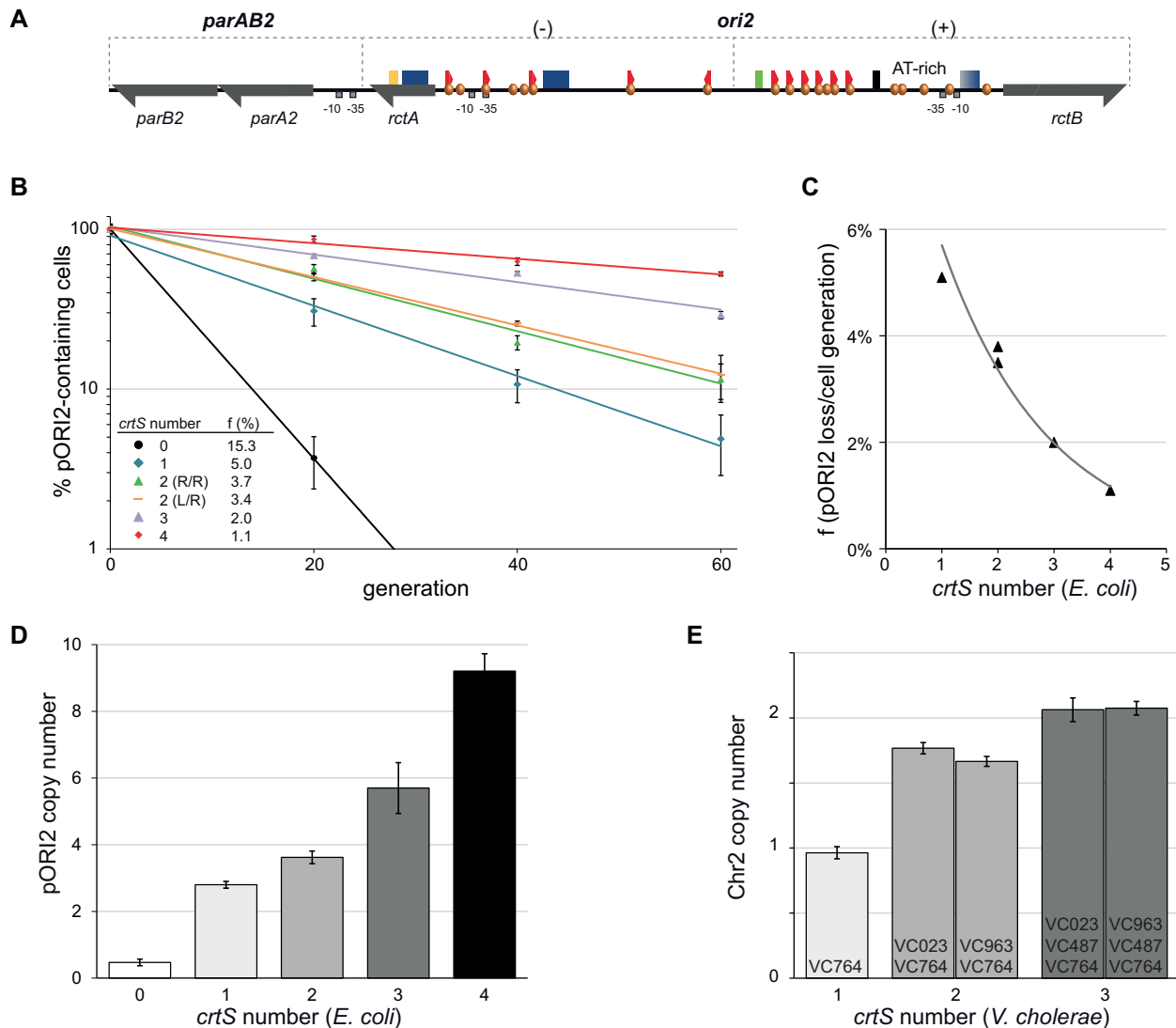
Figure 1. *crtS* controls Chr2 copy number. (**A**) Schematic map of the origin region of *V. cholerae* Chr2 (*ori2*) and of the contiguous *parA2* and *parB2* genes. *ori2* can be divided in two parts (+) and (−). The minimum functional origin (+) includes an array of six regular spaced iterons (red pentagons) oriented in a head-to-tail manner each containing a GATC Dam methylation site (orange spheres). It also contains an AT-rich region, putative binding sites for IHF (black rectangle) and DnaA (green rectangle), the *rctB* gene encoding for the initiator (grey half arrow). RctB auto-regulates its own expression through binding to a 29-mer (truncated 39-mer, rectangle with blue gradient) located in its promoter region (−35 and −10 sites are represented by grey squares). The negative regulatory region (−) includes two 39-mers (blue rectangles), five iterons (red pentagons) and the *rctA* non-translated ORF which harbors an iteron in its promoter and a 39-mer and a *parS2(-B)* site (yellow rectangle) within its coding sequence. (**B**) pORI2 plasmid loss in *E. coli* strains carrying up to four chromosomal *crtS* sites. f: frequency of pORI2 loss at each cell generation. 2(R/R), the two *crtS* sites are located on the same chromosomal arm. 2(L/R), the two *crtS* sites are located on different arms. Values are normalized by setting the first value of each series to a baseline of 100%. (**C**) Exponential increase of pORI2 stability (experimental values from B) as a function of *crtS* copy number in *E. coli* ($R^2 = 0.98$). (**D**) Histograms representing pORI2 copy number relative to the chromosome (pORI2/*oriC*) in *E. coli* strains carrying up to four chromosomal *crtS* sites. pORI2 and *oriC* copy number were measured by dPCR on genomic DNA from non-replicating cells (stationary phase) after 16hours growth with antibiotic selection for the plasmid. (E) Histograms representing Chr2 copy number relative to Chr1 (*ori1*/*ori2*) in *V. cholerae* strains carrying up to three chromosomal *crtS* sites. *ori1* and *ori2* copy number were measured by dPCR on genomic DNA from non-replicating cells (stationary phase) after 16 h growth. All the data represent the mean of three independent experiments (± standard deviation).

ditions, RctB formed a complex with *crtS* radiolabeled linear DNA (Figure 3A, 114 bp *crtS*). Since RctB preferentially binds to Dam methylated iterons (12) and the *crtS*-containing fragments has two very conserved GATC sites that can be Dam methylated, we compared the binding of RctB on *in vitro* methylated and unmethylated DNA substrates (Figure 3A, 114 bp *crtS* versus 114 bp *crtS*^Me). We observed that RctB could bind indistinguishably to both methylated and unmethylated *crtS*-containing DNA fragments with no apparent different efficiencies (Figure 3B, 114 bp *crtS* versus 114 bp *crtS*^Me). We confirmed these results *in vivo* in *V. cholerae* mutants with point mutations in *crtS* GATC motifs that showed no effect on *ori1*/*ori2* ratios compared to the WT (Supplementary Figure S7). These results allowed us to conclude that the methylation state of
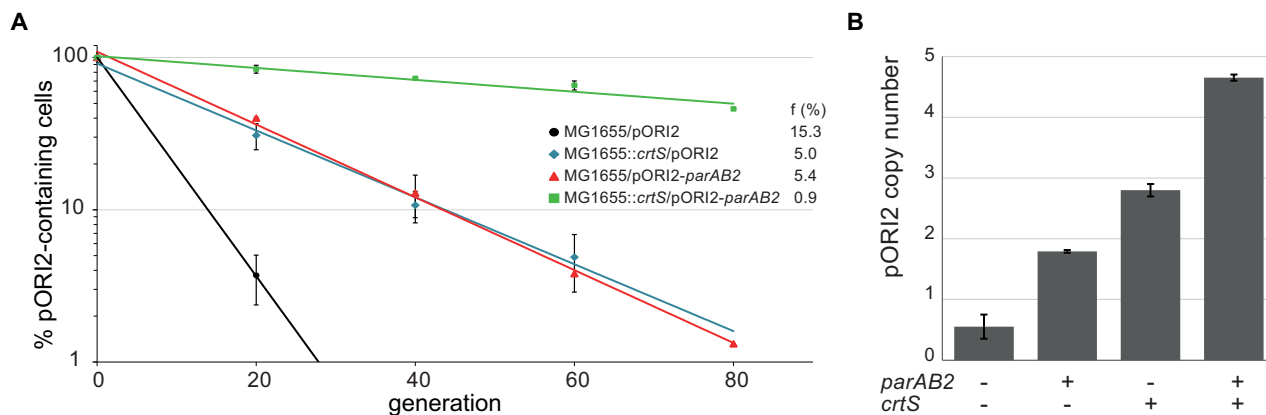
Figure 2. *crtS* and *parAB2* have an additive effect on the control of *ori2* copy number. (**A**) Loss of pORI2 (with or without *parAB2*) in *E. coli* strains (with or without a *crtS* site). f: frequency of plasmid loss at each cell generation. (**B**) Copy-number of pORI2 (with or without *parAB2*) relative to the chromosome (pORI2 /*oriC*) in *E. coli* strains (with or without a *crtS* site).
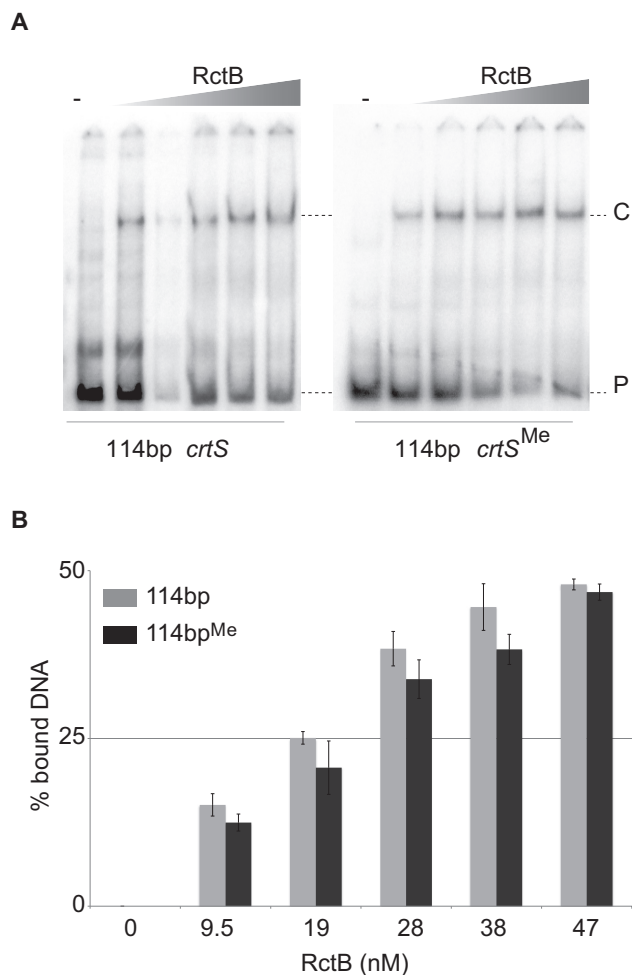

Figure 3. RctB directly binds to *crtS* independently of its methylation state. (**A**) EMSA experiment showing the interaction between increasing concentrations of RctB and *crtS*. The binding of RctB on either methylated (Me) or unmethylated 114bp *crtS* containing DNA probes is compared. Unbound DNA (P) and DNA complexed with RctB (C) are indicated. (**B**) Quantification of three independent experiments presented in (A), the concentrations in nanomolar (nM) of RctB are presented on the X-axis. Percent of bound DNA is equal to (intensity of the shifted band/combined intensities of shifted and unbound DNA band) × 100. The grey bars correspond to the unmethylated 114 bp *crtS* and the dark grey bars correspond to the methylated *crtS*.

crtS has no impact on either RctB binding nor its control on *ori2* replication initiation.

The *crtS* minimum functional site overlaps with RctB footprint

We next determined the minimum functional sequence of *crtS* by testing its activity on Chr2 replication in *V. cholerae*. To do so, we used a *crtS*-containing DNA fragment of 164bp and reduced it from both sides down to 58bp (Figure 4A, left panel). These fragments were inserted specifically in the Tn7 insertion site (*attTn7*) located on Chr1 of *V. cholerae*, prior excision of its own native site (Supplementary Figure S1). Using dPCR, we measured the copy number variation between Chr1 and Chr2 of non-replicating *V. cholerae* carrying the various *crtS* sizes (Figure 4A, right panel). If *crtS* is active in triggering Chr2 replication, we expect an *ori1/ori2* ratio ~1 (e.g. WT). If the active length of *crtS* is disrupted, Chr2 will be lost which will translate into a high *ori1/ori2* ratio (e.g. 58 bp fragment). Our results show that a 62 bp sequence is sufficient to keep an equal copy number of Chr1 and Chr2 in *V. cholerae* suggesting that the 62bp sequence is the minimum functional *crtS* site. The minimum *crtS* site doesn't contain any GATC sites, which corroborates with the fact that RctB does not require Dam methylation to bind to *crtS*. Moreover, the minimum *crtS* site does not contain the putative DnaA binding site (Supplementary Figure S8A) (22). We compared the binding of *V. cholerae* DnaA$_{Vc}$ to both *ori2* and *crtS* in the presence of ATP and observed that DnaA$_{Vc}$ binds to *ori2* but not to *crtS* (Supplementary Figure S8B). These results were confirmed *in vivo* in *V. cholerae* mutants with point mutations in the putative DnaA binding site of *crtS* (Supplementary Figure S8C). We conclude that the DnaA box-like motif on *crtS* is too degenerated (three mismatches to the consensus sequence) to bind DnaA (even in the presence of ATP) and should no longer be referred to as a DnaA box.

We next identified the RctB binding site within *crtS* by performing a DNase I footprinting experiment, where RctB-bound DNA is protected from DNase I cleavage, and we verified that the active 62bp *crtS* overlaps with this binding site. Using a non-methylated *crtS*-containing
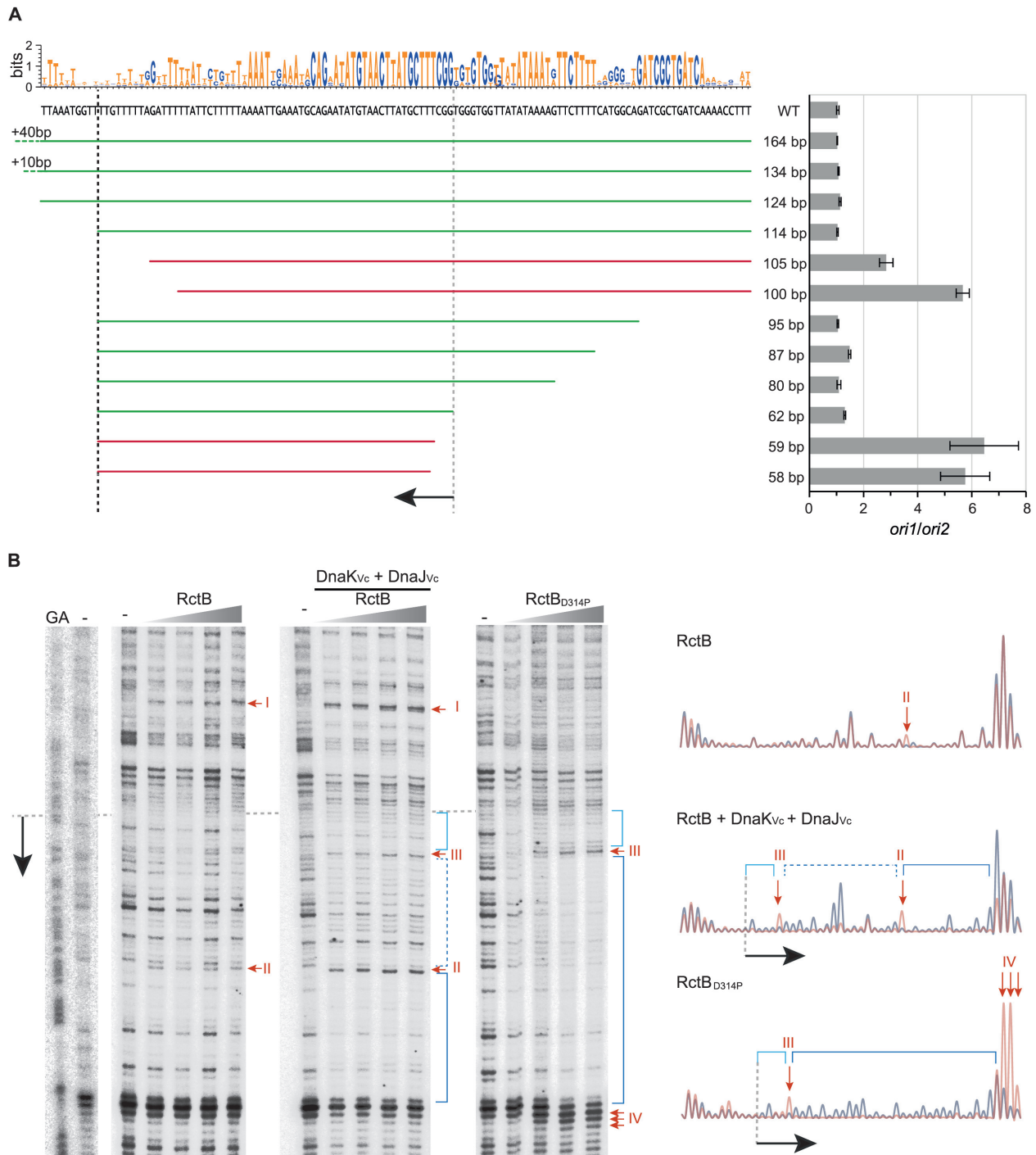
Figure 4. *crtS* minimum functional site in *V. cholerae* overlaps RctB binding site *in vitro*. (**A**) WebLogo illustration of the 124 bp consensus sequence surrounding *crtS* from 28 *Vibrionaceae* species published with complete assembled genomes on NCBI (Supplementary Figure S10). The heights of letters within the stack indicates the relative frequency of each base at that position. The sequence under the WebLogo corresponds to *V. cholerae* N16961 (WT) *crtS* sequence. Histograms representing *ori1/ori2* ratios measured by dPCR on the genomic DNA from non-replicating *V. cholerae* strains carrying various *crtS* sizes (from 164bp down to 58bp). Various length of *crtS* were inserted in *V. cholerae attTn7* site prior deleting the native *crtS* site (Supplementary Figure S1). Active *crtS* sites (*ori1/ori2* ~1) are represented by green lines. Inactive *crtS* sites (*ori1/ori2* > 1.5) are represented by red lines. *ori1* and *ori2* copy number were measured by dPCR on genomic DNA from non-replicating cells (stationary phase) after 16hours growth. All the data represent the mean of three independent experiments (+/− standard deviation). The two vertical grey dash lines indicate the limits of the minimum 62bp functional *crtS* site. (**B**) The DNase I footprinting experiment was performed with an identical increasing concentration of RctB and RctB$_{D314P}$ (from 20 to 100 nM), in the presence or absence of constant 5nM of DnaK$_{Vc}$ and 5nM of DnaJ$_{Vc}$ concentrations. From the left to the right: the G+A chemical sequencing ladder is presented near a digested sequence without protein, the footprint with RctB, RctB+DnaK/J$_{Vc}$ and RctB$_{D314P}$ and the right panel correspond to the quantification of the first (blue) and last (red) lines of each gel. The hypersensitive cleavage sites (I, II, III, IV) and the protected windows are indicated on the gels and the quantifications.

270 bp linear DNA substrate, we were able to detect a window of RctB-protected DNA, against the DNase I digestion (Figure 4B). With increasing amounts of RctB, we observed two hypersensitive DNase I cleavage sites (RctB, I and II). The presence of hypersensitive positions within the region protected by the bound protein indicates that binding of RctB induced deformation of the DNA at the binding site. Upon addition of DnaK$_{Vc}$ and DnaJ$_{Vc}$ chaperones, a region of protection extended from one cleavage site (RctB+DnaK/J$_{Vc}$, II) in both directions and unraveled a new DNase I hypersensitive cleavage site (RctB+DnaK/J$_{Vc}$, III). This result suggests that DnaK/J promote RctB binding to *crtS* and that the DNA bound by RctB is distorted. We further used a monomeric mutant of RctB where aspartate 314 is substituted by a proline residue (D314P) that disrupts the dimerization process (25). With RctB$_{D314P}$ mutant, the protected region was more discernable and flanked by additional DNase I hypersensitive cleavage sites (RctB$_{D314P}$, IV), and correctly correspond to the results observed with RctB+DnaK/J$_{Vc}$. We observed a 51bp-protected window with RctB+DnaK/J$_{Vc}$ and RctB$_{D314P}$, which largely overlaps with the 62bp minimum *crtS* site (Figure 4A, Supplementary Figure S6). Note that two hypersensitive cleavage sites (RctB+DnaK/J, I and II) disappear in RctB$_{D314P}$ footprint suggesting that RctB and RctB$_{D314P}$ binding on *crtS* are slightly different. Altogether, these results suggest that RctB preferentially binds to *crtS* as a monomer and that DnaK/J may promote RctB monomerization by remodeling, as already observed for Rep initiators (38).

RctB monomers bind to iteron, 39-mer and *crtS* prior oligomerization

To characterize the binding of RctB on *crtS*, we performed EMSA experiments on a 54 bp *crtS*-containing DNA probe including the 51 bp RctB footprint sequence (Supplementary Table S4). In the presence of increasing concentration of RctB and the 54 bp DNA probe, we observed at least two complexes: C2 and C3 (Figure 5A). We compared the migration of these complexes with RctB and RctB$_{D314P}$ bound to 54 bp linear DNA fragments containing a 39-mer motif. This allowed us to conclude that C2 corresponds to the binding of two RctB molecules on *crtS* and that the complex C3 is formed by the binding of a third RctB molecule (Figure 5A). Note that C2 complexes formed by RctB and RctB$_{D314P}$ harbor a slight shift of migration, possibly due to the different conformations of the complex, also observed in footprinting experiments (Figures 4B and 5A). At higher concentration of RctB (+DnaKJ$_{Vc}$) and RctB$_{D314P}$, an additional complex appeared, C4, which is probably due to the binding of a fourth RctB molecule. Upon the addition of DnaK$_{Vc}$ and DnaJ$_{Vc}$ and with increasing concentration of RctB$_{D314P}$, the C3 and C4 complexes appeared earlier (Figure 5A). The quantification of the EMSA experiments showed that RctB binding to *crtS* was more efficient in presence of DnaK/J$_{Vc}$ or when RctB is present only as a monomer (RctB$_{D314P}$) (Figure 5A). Taken together, these results in agreement with the results obtained from the footprint (Figure 4B), allowed us to conclude that RctB binds to *crtS* as a monomer. These same results suggest also that the chaperones, in addition to monomerization of RctB, enhance the oligomerization of RctB onto the DNA.

We next verified this activity on the methylated iteron and 39-mer (Figure 5B). In presence of RctB or RctB$_{D314P}$, the shifted bands of the probes carrying one iteron or one 39-mer corresponding to C1 and C2 showed an identical migration. Furthermore, RctB$_{D314P}$ showed a higher efficiency to bind the two different sites. These results suggest that RctB binds to the iterons and the 39-mer only as a monomer. At the higher RctB$_{D314P}$ concentration a third band: C3 can be observed. When DnaK/J$_{Vc}$ are added to the reaction with either RctB or RctB$_{D314P}$, the C3 complex is observed at all concentrations and has become majoritarian, suggesting an activation of the RctB oligomerization by DnaK/J$_{Vc}$, as it is the case with crtS. Note that we confirmed the absence of RctB binding to a random DNA sequence as well as the absence of DnaK/J$_{Vc}$ binding to RctB binding sites (Supplementary Figure S9A).

We wondered if RctB oligomerization onto DNA is dependent on protein/DNA or on protein/protein interactions. To address this question, we used two iteron-containing probes with different flanking sequences (Supplementary Table S4). EMSA experiments show that RctB ($\pm$ DnaK/J$_{Vc}$) form C1, C2 and C3 complexes on both methylated iteron-containing probes (Supplementary Figure S9B). This suggests that RctB binds specifically to the iteron site and spreads non-specifically to flanking DNA. We further used a RctB mutant deleted for its domain 4, which is supposedly involved in protein/protein interactions (17,25). EMSA experiments show that RctB$_{\Delta IV}$ ($\pm$ DnaK/J$_{Vc}$) mostly form the C1 complex, while complexes C2 and C3 nearly completely disappeared. Further quantification showed that DnaK/J$_{Vc}$ are still able to enhance RctB$_{\Delta IV}$ binding to iterons, increasing only C1 formation. This suggests that RctB$_{\Delta IV}$ is still monomerized by DnaK/J$_{Vc}$, but unable to oligomerize on the DNA. Taken together these results allowed us to conclude that DnaK and DnaJ are involved in two steps of RctB modification. DnaK/J promote the transfer of RctB from its dimeric to its monomeric form and also modify the RctB monomer to enhance its oligomerization onto the DNA, which is mediated by the domain 4 of RctB.

DISCUSSION

crtS controls Chr2 copy number

In our previous study, we looked at the role of *crtS* in replicating cells (33). We observed that the timing of replication of *crtS* determines the timing of initiation of Chr2. Hence the location of *crtS* compared to *ori1* was important in controlling the timing of Chr2 replication. However, we did not look at the role of *crtS* on Chr2 copy number control. In this study, we measured *ori1*:*ori2* ratios in non-replicating cells to infer the number of Chr2 relative to Chr1. In wild-type *V. cholerae* with a unique *crtS* site, non-replicating cells have an equal number of Chr1 and Chr2 (Figure 4A, WT). When *crtS* is moved closer to *ori1* in the *attTn7* site (VC487), we observed an equal number of Chr1 and Chr2 like in WT (Figure 4A, 164 bp). Therefore the location of *crtS* compared to *ori1* has no impact on Chr2 copy number. When we increase the number of *crtS* sites, this balance is altered and
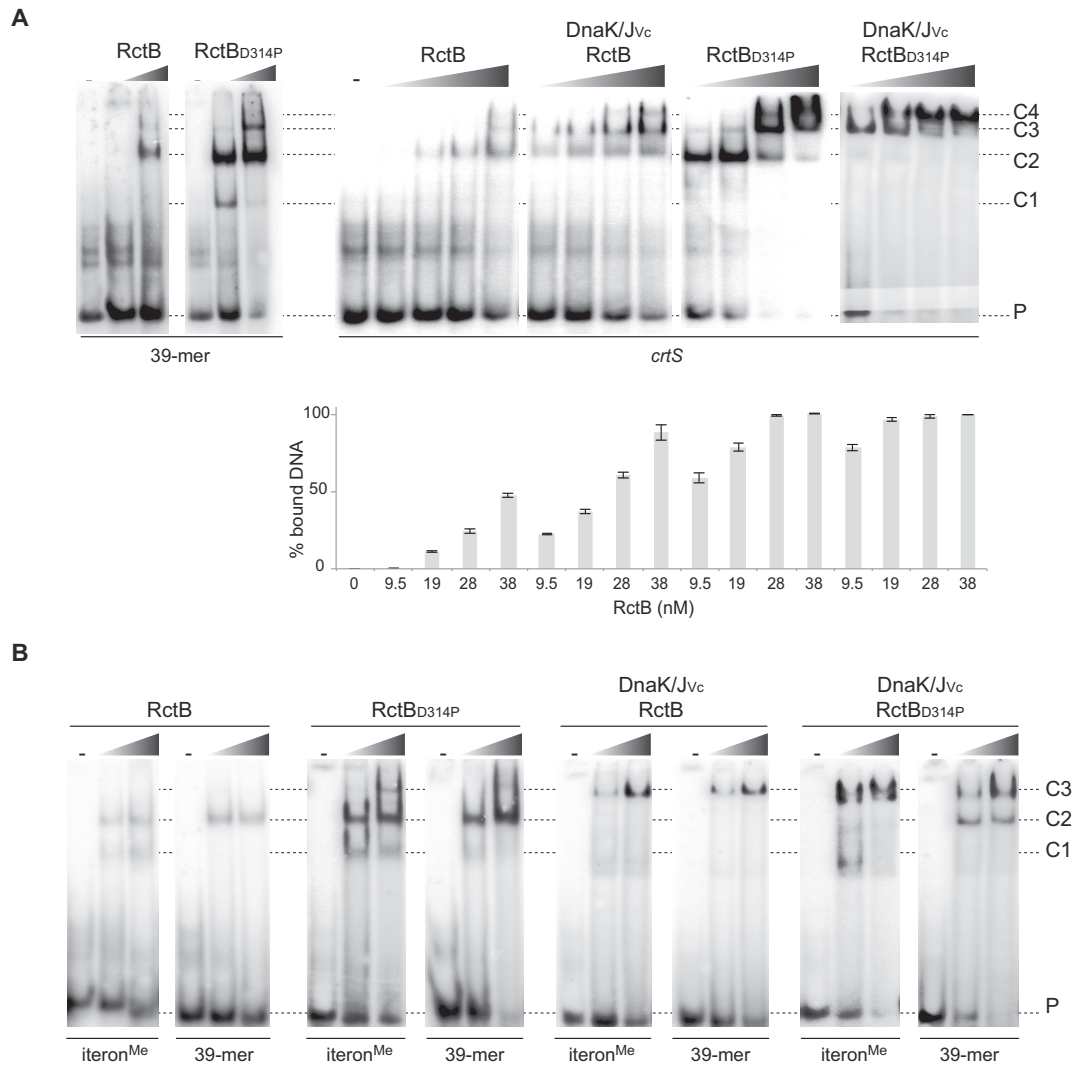
Figure 5. Multiple monomers of RctB bind to *crtS*, iterons and 39-mers. (**A**) EMSA experiments with 54bp DNA probes carrying either a 39-mer or a *crtS* site. The unbound DNA (**P**) and RctB/DNA complexes (C1, C2, C3 and C4) are indicated. The C1, C2, C3 and C4 complexes correspond to the binding of 1, 2, 3 and 4 RctB molecules, respectively. Histograms correspond to the quantification of three independent experiments with the 54bp-*crtS* DNA probe. RctB concentration are indicated on the x-axis with the same constant DnaK/J_{Vc} concentrations as Figure 4B. (**B**) Comparison of results obtained by EMSA experiments using 40bp probes carrying one methylated iteron (12-mer) or one 39-mer. RctB and RctB$_{D314P}$ concentrations were 19 and 38 nM, respectively. Remaining details are the same as those described in A.

Chr2 number exceeds Chr1 number (Figure 1). Whether we added a second site near the origin or the terminus of Chr1, the effect was the same on *ori1/ori2* ratios (Figure 1E, VC023 versus VC963). This confirms that *crtS* location has no effect on Chr2 copy number. In absence of a functional *crtS*, Chr2 copy number relative to Chr1 dramatically drops (Figure 4, 58 bp) which is coherent with Chr2 loss already observed in a population of *crtS* deleted mutants (33). Having a unique copy of *crtS* is important to maintain an equal ratio of Chr1 and Chr2 suggesting that *crtS* limits Chr2 replication to one round per cell generation. This study demonstrates that *crtS* not only controls the timing of initiation of Chr2 but also regulates its copy number.

We also observed in *E. coli*, that by adding up to four chromosomal copies of *crtS*, we gradually increased the copy number of an *ori2*-driven plasmid (pORI2). This demonstrates that just by providing *crtS* and *ori2* in *E. coli*,

we can reconstitute a controlled replication system where the copy number of an *ori2*-driven plasmid will depend on the number of *crtS* chromosomal sites. When a fifth copy of *crtS* was inserted in the *E. coli* chromosome, pORI2 copy number varied from 10 to 40 copies suggesting that above 4 *crtS* sites, the control of plasmid replication is less tightly regulated (data not shown). Note that we also observed very inconsistent results when providing *crtS* on a plasmid in *E. coli*. Moreover *crtS* on a plasmid doesn't fully complement a *crtS* deleted mutant of *V. cholerae* (data not shown). We further observed that *crtS* and *parAB2* have an additive effect on the control of pORI2 copy number (Figure 2B). Indeed in the presence of a single *crtS* site, an *ori2*-driven plasmid with a partition system (ParAB2, *parS2*) is very stable with <1% loss per cell generation (Figure 2A). The cumulative stabilisation effect of *crtS* and *parAB2* is higher than the cumulative effect of four *crtS* sites in ab-

sence of *parAB2* (Figures 1B and 2A). This ability of *crtS* to regulate pORI2 copy number displays obvious interesting potentials for biotechnological applications such as controlling the dosage of genes of interest encoded on an *ori2*-driven plasmid by modifying the *E. coli* host (carrying various number of *crtS*) or keeping an artificial plasmid stable without requiring for antibiotic selection.

Furthermore, we saw an important difference between *E. coli* and *V. cholerae* in the *crtS*-mediated control of *ori2* copy number. While we observed a high increase of pORI2 copy number as a function of *crtS* number in *E. coli*, Chr2 copy number seemed to reach a plateau (ori2/ori1 ∼2) in *V. cholerae* (Supplementary Figure S4B). This suggests that Chr2 copy number is restricted in *V. cholerae*. This could be explained by the physiological burden of having multiple Chr2 (e.g. higher dosage of toxic genes, such as the presence of 18 toxin–antitoxin modules on Chr2) (39). However, we didn't see any fitness or morphological defects in *V. cholerae* mutants carrying two or three *crtS* sites (data not shown). We can also envisage that sister chromatids have to compete for limiting replication factors, such as proteins responsible for replication initiation and/or pools of precursors that are required for DNA synthesis. Another plausible explanation is the presence on Chr2 of a locus located 40 kb away from *ori2* which negatively regulates replication at *ori2* (22).

Another observation is that Chr2 copy number doesn't increase linearly. For example, the *ori2*/*ori1* ratio of non-replicating *V. cholerae* with two *crtS* sites equals ∼1.7, a decimal number. This suggests the existence of heterogeneity in the population with cells containing more chromosomes than others. We previously observed cell-to-cell variation in the replication dynamics of *V. cholerae* with two *crtS* sites (asymmetric cell division resulting in daughter cells that differ in both size and Chr2 copy number) (33). We speculate that this heterogeneity may reflect a relaxation of the cell cycle due a disorder in the replication checkpoint.

crtS minimum functional site

Since we observed *ori2* replication control discrepancies between *E. coli* and *V. cholerae* or between an *ori2*-driven plasmid and Chr2, we decided to determine the minimum active *crtS* sequence in its native host on the chromosome. We found a minimum active chromosomal *crtS* sequence of 62bp in *V. cholerae*. This minimum 62bp *crtS* site largely overlaps with the 51bp-protected window obtained with RctB+DnaK/J$_{Vc}$ and RctB$_{D314P}$ binding to *crtS* (Figure 4B, Supplementary Figure S6). Surprisingly, some DNA motifs outside the minimum *crtS* site are very conserved (Supplementary Figure S10) and for this reason these motifs were expected to be important. However, their deletion or mutation have no consequences on *crtS* activity (Supplementary Figures S6–S8). The minimum 62 bp *crtS* site excludes all the conserved GATC methylation sites, suggesting that Dam methylation is not playing a role in the *crtS* mediated activation of *ori2* upon passage of the replication fork (Figure 4). This was confirmed by mutating the GATC sites upstream and downstream of the 62 bp (Supplementary Figure S7). Furthermore, we showed that RctB indifferently binds to methylated and non-methylated *crtS* sequences (Figure 3). The minimum 62bp *crtS* site also excludes the putative DnaA box. We further mutated this box and confirmed that it is not important for *crtS* activity. The *crtS* putative DnaA-box has three mismatches compared to the *ori1* and *ori2* DnaA boxes. We show that DnaA does not bind to *crtS in vitro* (Supplementary Figure S8), indicating that this putative box is too degenerated to permit the binding of DnaA. This confirms previous results observed in an *E. coli* DnaA temperature-sensitive mutant, where pORI2 plasmid could still replicate at 42°C (22). On the other hand, we show here the first evidence of DnaA binding to *ori2* (Supplementary Figure S8). The DnaA box found in *ori2* was shown to be essential to initiate Chr2 replication (14). Nevertheless, the exact implication of DnaA in *ori2* replication control is still unknown. From our knowledge on the replication control of iteron-containing plasmids, we can hypothesize that DnaA could be implicated in the stabilization of the RctB complex opening the A-T rich region, or could be involved in the recruitment of the other replisome components (40).

This 62bp minimum sequence is different from the 70bp minimum *crtS* site found in *E. coli* (22). Both sequences only partially overlap (Supplementary Figure S6). It appears that the 11bp upstream of the 70bp is crucial for *crtS* proper activity in *V. cholerae* and not important in *E. coli*. On the other hand, the *crtS* putative DnaA box is essential in *E. coli* but is not important in *V. cholerae* for *crtS* activity (Figure 4, Supplementary Figure S6). Multiple reasons could explain why the *crtS* minimum sequences differ such as the use of different hosts, the use of an artificial plasmid system to test *ori2* replication and the use of a plasmid containing *crtS* in *E. coli* instead of using a chromosomal site.

DnaK/J promote both RctB monomerization and additional binding of RctB monomers

The RctB binding activity to *crtS* allowing to correctly characterize this interaction was never shown and we provide here the first characterization of their direct interaction.

By comparing the binding of RctB and RctB$_{D314P}$ on *crtS*, we clearly observed that RctB preferentially binds to *crtS* as a monomer (Figure 5A). Furthermore, we observed the same for RctB binding activity to iterons and 39-mer. In Figure 5B, the C1 and C2 complexes formed by RctB and RctB$_{D314P}$ on iterons and 39-mer harbor an identical migration shift. All these results, along with the RctB structural data (25,27), allow us to say that RctB binds to iterons, 39-mers and *crtS* preferentially under its monomeric form. Besides, the region of protection, in presence of RctB$_{D314P}$ and RctB+DnaK/J, is too large for the binding of one monomer suggesting that more than one RctB binds to *crtS*. However, we also observed a C1 slight shift of migration between RctB and RctB$_{D314P}$ using 54bp probes (39-mer and *crtS*). Thus, without structural study of the RctB/DNA complexes, we cannot completely exclude that RctB dimers could weakly bind to DNA.

In all cases, the presence of *V. cholerae* DnaK and DnaJ increased the efficiency of RctB binding to its DNA substrates (Figure 5). In iteron-containing plasmids, the chaperones favor monomerization of plasmid initiators and thereby increase monomer binding to the origin. However, monomers also need to be remodeled to promote

iteron binding (38). This could also be the case for RctB. Indeed, the addition of DnaK/J$_{Vc}$ led to the apparition of an additional complex formed by RctB binding to its recognition sites (Figure 5B). This was also observed with RctB$_{D314P}$, suggesting the DnaK/J$_{Vc}$ do not only favor RctB monomerization but also remodel RctB to form higher order complexes. We propose that DnaK/J may re-model RctB monomers to further promote the binding of additional RctB monomers by oligomerization on DNA. Indeed, we saw that the number of additional DNA/RctB complexes (C1, C2, C3 and C4) depends on the length of the DNA containing the RctB-binding site (40bp vs. 54bp) and not on the sequence (Figure 5, Supplementary Figure S9). RctB$_{\Delta IV}$ mutant was enabled to form com-plexes C2 and C3 using a 40bp-methylated iteron, mean-ing that the RctB oligomeric state onto DNA is mediated by a protein/protein interaction involving domain 4. RctB seems to harbor two types of protein/protein interaction, a dimeric state and an oligomeric state mediated by domains 2 and 4 respectively.

Such observations on RctB binding upon the addition of DnaK/J$_{Vc}$ were never reported. In our experiments we used purified *V. cholerae* DnaK$_{Vc}$ and DnaJ$_{Vc}$, while to our knowledge, previous reported studies were done using DnaK$_{Ec}$ and DnaJ$_{Ec}$ from *E. coli*. Comparing the sequences of DnaK from *E. coli* and from *V. cholerae* reveals that the C-terminal extremities of both proteins share only 62% identity. This observation suggests that species-specific in-teractions between DnaK$_{Vc}$ and RctB allow for the *in vitro* observation of RctB remodeling that is not observed using the *E. coli* chaperones. Furthermore, when pORI2 is used in *E.coli* plasmid stability assays, RctB binding activity is un-der the control of DnaK/J$_{Ec}$, which could take part to the differences observed between *ori2* copy number increasing induced by *crtS* in *V. cholerae* and in *E. coli*.

In *V. cholerae*, it appears that the chaperones DnaK and DnaJ are the master regulator of the RctB interac-tion with its binding sites. Whatever the site, RctB has to be monomerized by DnaK/J to enhance its binding ac-tivity. On all its substrates, we show that RctB specifically binds under its monomeric form (Figure 5). It appears that DnaK/J promotes the non-specific binding of additional RctB monomers (Figure 5B, Supplementary Figure S9). To sum up, DnaK/J could remodel RctB monomers to pro-mote their oligomerization onto DNA after their initial binding.

New insights into *crtS* mode of action

Two parameters play a major role in Chr2 replication con-trol by *crtS*: 1) The location of *crtS* on Chr1 determines Chr2 timing of replication; 2) the number of *crtS* sites de-termines the copy number of Chr2. From our *in vitro* study, we propose that RctB monomers oligomerize on Chr1 from *crtS* (the nucleation site) and further trigger Chr2 replica-tion by a replication-dependent mechanism that is still un-clear. Theoretically, the increase in *crtS* copy number or change of its conformation during replication could pro-mote a signal for Chr2 to initiate. Passage of the repli-cation fork across *crtS* would generate transiently hemi-methylated GATC that could affect RctB binding. Though,

we ruled out this hypothesis by demonstrating that both the methylation of *crtS* and the presence of GATC motifs have no impact on RctB binding and Chr2 replication con-trol, respectively. Passage of the replication fork across *crtS* would also generate single stranded DNA on the template for lagging-strand synthesis which may affect RctB binding. We showed that RctB binds to double stranded *crtS in vitro*. The replisome could dislocate and/or remodel *crtS*-bound RctB molecules. Finally, we showed that the augmentation of *crtS* sites increases the copy number of *ori2*-driven plas-mids in non-replicating *E. coli* and the copy number of Chr2 in non-replicating *V. cholerae*. Therefore, the duplication of *crtS* sites during replication could be the signal that triggers Chr2 replication. Indeed, a recent study shows that the *crtS* duplication could be sufficient to initiate *ori2* replication ini-tiation (41).

In this study, we show that Chr2 copy number increases when additional *crtS* sites are supplied in *trans*. This is the opposite of the impact on plasmid copy number of adding iterons in *trans*. A supply of additional iterons in *trans* de-creases plasmid copy number (42). This is due to their titra-tion activity of the initiator, leaving less of the initiator avail-able for binding to the origin. A titration mechanism of RctB by *crtS* would fire both *ori2* upon release of RctB. Here, we show that it is not the case for *crtS* and that *crtS* mode of action is probably not mediated by the titration of RctB molecules. This fits with our previous results showing that the duplication of one *crtS* triggers the firing of only one *ori2* (33). Chr2 initiation firing probably necessitates a direct interaction between *crtS* and *ori2* which could be me-diated by RctB. Such a contact was observed between *ori2* and Chr1 by 3C and may be caused by the simultaneous binding of RctB to *ori2* and *crtS* (33). However, further ex-perimental data are needed to understand *crtS* mode of ac-tion.

REFERENCES

1. diCenzo,G.C. and Finan,T.M. (2017) The divided bacterial Genome: Structure, function, and evolution. *Microbiol. Mol. Biol. Rev.: MMBR*, **81**, e00019-17.
2. Harrison,P.W., Lower,R.P., Kim,N.K. and Young,J.P. (2010) Introducing the bacterial 'chromid': Not a chromosome, not a plasmid. *Trends Microbiol.*, **18**, 141–148.
3. Touchon,M. and Rocha,E.P. (2016) Coevolution of the organization and structure of prokaryotic genomes. *Cold Spring Harbor Perspect. Biol.*, **8**, a018168.
4. Nordstrom,K. and Dasgupta,S. (2006) Copy-number control of the *Escherichia coli* chromosome: A plasmidologist's view. *EMBO Rep.*, **7**, 484–489.
5. Val,M.E., Soler-Bistue,A., Bland,M.J. and Mazel,D. (2014) Management of multipartite genomes: The *Vibrio cholerae* model. *Curr. Opin. Microbiol.*, **22**, 120–126.
6. Espinosa,E., Barre,F.X. and Galli,E. (2017) Coordination between replication, segregation and cell division in multi-chromosomal bacteria: lessons from *Vibrio cholerae*. *Int. Microbiol.*, **20**, 121–129.
7. Ramachandran,R., Jha,J., Paulsson,J. and Chattoraj,D. (2017) Random versus Cell Cycle-RegulatedReplication Initiation in Bacteria: Insights from Studying Vibrio choleraeChromosome 2. *Microbiology and molecular biology reviews : MMBR*, **81**, e00033-16.
8. Egan,E.S. and Waldor,M.K. (2003) Distinct replication requirements for the two *Vibrio cholerae* chromosomes. *Cell*, **114**, 521–530.
9. Hansen,F.G. and Atlung,T. (2018) The DnaA tale. *Front. Microbiol.*, **9**, 319.
10. Katayama,T., Ozaki,S., Keyamura,K. and Fujimitsu,K. (2010) Regulation of the replication cycle: conserved and diverse regulatory systems for DnaA and *oriC*. *Nat. Rev.. Microbiol.*, **8**, 163–170.
11. Koch,B., Ma,X. and Lobner-Olesen,A. (2010) Replication of *Vibrio cholerae* chromosome I in *Escherichia coli*: dependence on *dam* methylation. *J. Bacteriol.*, **192**, 3903–3914.
12. Demarre,G. and Chattoraj,D.K. (2010) DNA adenine methylation is required to replicate both *Vibrio cholerae* chromosomes once per cell cycle. *PLoS Genet.*, **6**, e1000939.
13. Duigou,S., Yamaichi,Y. and Waldor,M.K. (2008) ATP negatively regulates the initiator protein of *Vibrio cholerae* chromosome II replication. *Proc. Natl. Acad. Sci. U.S.A.*, **105**, 10577–10582.
14. Gerding,M.A., Chao,M.C., Davis,B.M. and Waldor,M.K. (2015) Molecular dissection of the essential features of the origin of replication of the second *Vibrio cholerae* chromosome. *mBio*, **6**, e00973.
15. Schallopp,N., Milbredt,S., Sperlea,T., Kemter,F.S., Bruhn,M., Schindler,D. and Waldminghaus,T. (2017) Establishing a system for testing replication inhibition of the *Vibrio cholerae* secondary chromosome in *Escherichia coli*. *Antibiotics*, **7**, E3.
16. Venkova-Canova,T. and Chattoraj,D.K. (2011) Transition from a plasmid to a chromosomal mode of replication entails additional regulators. *Proc. Natl. Acad. Sci. U.S.A.*, **108**, 6199–6204.
17. Jha,J.K., Demarre,G., Venkova-Canova,T. and Chattoraj,D.K. (2012) Replication regulation of *Vibrio cholerae* chromosome II involves initiator binding to the origin both as monomer and as dimer. *Nucleic Acids Res.*, **40**, 6026–6038.
18. Venkova-Canova,T., Srivastava,P. and Chattoraj,D.K. (2006) Transcriptional inactivation of a regulatory site for replication of *Vibrio cholerae* chromosome II. *Proc. Natl. Acad. Sci. U.S.A.*, **103**, 12051–12056.
19. Venkova-Canova,T., Baek,J.H., Fitzgerald,P.C., Blokesch,M. and Chattoraj,D.K. (2013) Evidence for two different regulatory mechanisms linking replication and segregation of Vibrio cholerae chromosome II. PLoS Genet., **9**, e1003579.
20. Yamaichi,Y., Fogel,M.A. and Waldor,M.K. (2007) par genes and the pathology of chromosome loss in *Vibrio cholerae*. *Proc. Natl. Acad. Sci. U.S.A.*, **104**, 630–635.
21. Yamaichi,Y., Gerding,M.A., Davis,B.M. and Waldor,M.K. (2011) Regulatory cross-talk links *Vibrio cholerae* chromosome II replication and segregation. *PLoS Genet.*, **7**, e1002189.
22. Baek,J.H. and Chattoraj,D.K. (2014) Chromosome I controls chromosome II replication in *Vibrio cholerae*. *PLoS Genet.*, **10**, e1004184.
23. Kitagawa,R., Ozaki,T., Moriya,S. and Ogawa,T. (1998) Negative control of replication initiation by a novel chromosomal locus exhibiting exceptional affinity for *Escherichia coli* DnaA protein. *Genes Dev.*, **12**, 3032–3043.
24. Kasho,K. and Katayama,T. (2013) DnaA binding locus *datA* promotes DnaA-ATP hydrolysis to enable cell cycle-coordinated replication initiation. *Proc. Natl. Acad. Sci. U.S.A.*, **110**, 936–941.
25. Orlova,N., Gerding,M., Ivashkiv,O., Olinares,P.D., Chait,B.T., Waldor,M.K. and Jeruzalmi,D. (2017) The replication initiator of the cholera pathogen's second chromosome shows structural similarity to plasmid initiators. *Nucleic Acids Res.*, **45**, 3724–3737.
26. Jha,J.K., Ghirlando,R. and Chattoraj,D.K. (2014) Initiator protein dimerization plays a key role in replication control of *Vibrio cholerae* chromosome 2. *Nucleic Acids Res.* **42**, 10538–10549.
27. Jha,J.K., Li,M., Ghirlando,R., Miller Jenkins,L.M., Wlodawer,A. and Chattoraj,D. (2017) The DnaK chaperone uses different mechanisms to promote and inhibit replication of *Vibrio cholerae* chromosome 2. *mBio*, **8**, e00427-17.
28. Fournes,F., Val,M.E., Skovgaard,O. and Mazel,D. (2018) Replicate Once Per Cell Cycle: ReplicationControl of Secondary Chromosomes. *Front. Microbiol.*, **9**, 1833.
29. Demarre,G. and Chattoraj,D.K. (2010) DNA adenine methylation is required to replicate both *Vibrio cholerae* chromosomes once per cell cycle. *PLoS Genet.*, **6**, e1000939.
30. Val,M.E., Kennedy,S.P., Soler-Bistue,A.J., Barbe,V., Bouchier,C., Ducos-Galand,M., Skovgaard,O. and Mazel,D. (2014) Fuse or die: How to survive the loss of Dam in *Vibrio cholerae*. *Mol. Microbiol.*, **91**, 665–678.
31. Venkova-Canova,T., Saha,A. and Chattoraj,D.K. (2012) A 29-mer site regulates transcription of the initiator gene as well as function of the replication origin of *Vibrio cholerae* chromosome II. *Plasmid*, **67**, 102–110.
32. Rasmussen,T., Jensen,R.B. and Skovgaard,O. (2007) The two chromosomes of *Vibrio cholerae* are initiated at different time points in the cell cycle. *EMBO J.*, **26**, 3124–3131.
33. Val,M.E., Marbouty,M., de Lemos Martins,F., Kennedy,S.P., Kemble,H., Bland,M.J., Possoz,C., Koszul,R., Skovgaard,O. and Mazel,D. (2016) A checkpoint control orchestrates the replication of the two chromosomes of *Vibrio cholerae*. *Sci. Adv.*, **2**, e1501914.
34. Kemter,F.S., Messerschmidt,S.J., Schallopp,N., Sobetzko,P., Lang,E., Bunk,B., Sproer,C., Teschler,J.K., Yildiz,F.H., Overmann,J. et al. (2018) Synchronous termination of replication of the two chromosomes is an evolutionary selected feature in Vibrionaceae. *PLoS Genet.*, **14**, e1007251.
35. Dalia,A.B., McDonough,E. and Camilli,A. (2014) Multiplex genome editing by natural transformation. *Proc. Natl. Acad. Sci. U.S.A.*, **111**, 8937–8942.
36. McKenzie,G.J. and Craig,N.L. (2006) Fast, easy and efficient: site-specific insertion of transgenes into enterobacterial chromosomes using Tn*7* without need for selection of the insertion event. *BMC Microbiol.*, **6**, 39.
37. Madic,J., Zocevic,A., Senlis,V., Fradet,E., Andre,B., Muller,S., Dangla,R. and Droniou,M.E. (2016) Three-color crystal digital PCR. *Biomol. Detect. Quantifi.*, **10**, 34–46.
38. Dibbens,J.A., Muraiso,K. and Chattoraj,D.K. (1997) Chaperone-mediated reduction of RepA dimerization is associated with RepA conformational change. *Mol. Microbiol.*, **26**, 185–195.
39. Iqbal,N., Guerout,A.M., Krin,E., Le Roux,F. and Mazel,D. (2015) Comprehensive functional analysis of the 18 *Vibrio cholerae* N16961 Toxin-Antitoxin systems substantiates their role in stabilizing the superintegron. *J.Bacteriol.*, **197**, 2150–2159.
40. Konieczny,I., Bury,K., Wawrzycka,A. and Wegrzyn,K. (2014) Iteron plasmids. *Microbiol. Spectrum*, **2**, 6.
41. Ramachandran,R., Ciaccia,P.N., Filsuf,T.A., Jha,J.K. and Chattoraj,D. (2018) Chromosome 1 licenses chromosome 2 replication in Vibrio cholerae by doubling the crtS gene dosage. *PLoS genetics*, **14**, e1007426.
42. Pal,S.K., Mason,R.J. and Chattoraj,D.K. (1986) P1 plasmid replication. Role of initiator titration in copy number control. *J. Mol. Biol.*, **192**, 275–285.